On the refractive index for a nonmagnetic two–component medium: resolution of a controversy

Joseph B. Geddes III[1]
Beckman Institute for Advanced Science and Technology, University of Illinois at Urbana-Champaign, 405 North Mathews Avenue, Urbana, IL 61801, USA

Tom G. Mackay[2]
School of Mathematics, University of Edinburgh, Edinburgh EH9 3JZ, UK

Akhlesh Lakhtakia[3]
CATMAS — Computational & Theoretical Materials Sciences Group
Department of Engineering Science and Mechanics
Pennsylvania State University, University Park, PA 16802–6812, USA

Abstract

The refractive index of a dielectric medium comprising both passive and inverted components in its permittivity was determined using two methods: (i) in the time domain, a finite–difference algorithm to compute the frequency–domain reflectance from reflection data for a pulsed plane wave that is normally incident on a dielectric half–space, and (ii) in the frequency domain, the deflection of an obliquely incident Gaussian beam on transmission through a dielectric slab. The dielectric medium was found to be an active medium with a negative real part for its refractive index. Thereby, a recent controversy in the scientific literature was resolved.

Keywords: Active medium; Negative refraction; Time–domain analysis; Frequency–domain analysis

1 Introduction

A complex number $z = \psi\, e^{i\phi}$ possesses two square roots: $\sqrt{z} = \pm|\sqrt{\psi}|\, e^{i(\phi/2)}$. This presents a problem when a physical quantity (e.g., refractive index) is expressed as the square root of another physical quantity (relative permittivity). Which root is the physical one?

Our work grows out of a recent controversy over this question in the context of negative refraction of electromagnetic plane waves. Chen, Fischer, and Wise (CFW) considered an isotropic nonmagnetic medium with a relative permittivity scalar

$$\tilde{\epsilon}\,(\omega) = 1 + \sum_{\ell=1}^{2} \alpha_\ell \omega_\ell^2 \left[\omega_\ell^2 - (\omega + i\beta_\ell\omega_\ell)^2\right]^{-1}, \tag{1}$$

as a function of the angular frequency ω [1]. Herein, the constants $\alpha_1 = 2.4401$, $\alpha_2 = -0.14348$, $\beta_1 = 0.028571$, $\beta_2 = 0.020000$, $\omega_1 = 2.6371 \times 10^{15}$ rad s^{-1} and $\omega_2 = 3.7673 \times 10^{15}$ rad s^{-1}.

[1]Corresponding Author. Email: geddes@uiuc.edu
[2]Email: T.Mackay@ed.ac.uk.
[3]Email: akhlesh@psu.edu

The permittivity scalar comprises a passive and an inverted component. Most importantly, for $\lambda_0 \in [445, 535]$ nm, where λ_0 denotes the free–space wavelength, $\mathrm{Im}(\tilde{\epsilon}) < 0$, as shown in Fig. 1; here and hereafter, an $\exp(-i\omega t)$ time–dependence is implicit for all frequency–domain field phasors.

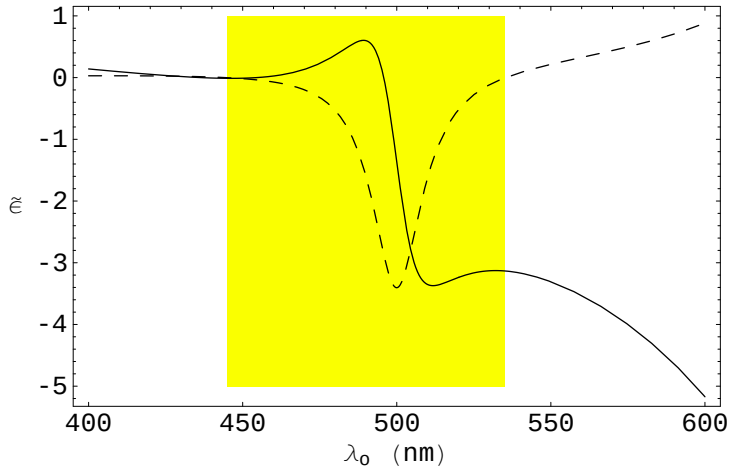

Figure 1: Real (solid) and imaginary (dashed) parts of $\tilde{\epsilon}$ plotted against free–space wavelength (in nm).

CFW deduced that for $\lambda_0 \in [445, 535]$ nm, the refractive index $n = \sqrt{\tilde{\epsilon}}$ must be such that $\mathrm{Re}(n) < 0$ and $\mathrm{Im}(n) > 0$. This deduction stemmed from the premise that the phase angle of $\tilde{\epsilon}$ is a continuous function of λ_0, which has been supported by certain recent theoretical arguments [2, 3]. Accordingly, CFW argued that their medium could refract negatively.

Alternatively, on the basis that (i) energy flow grows along the direction of propagation when $\mathrm{Im}(\tilde{\epsilon}) < 0$ [4]; or (ii) the real part of the wave impedance is positive–valued on the grounds of causality [5], it may be deduced that $\mathrm{Re}(n) > 0$ and $\mathrm{Im}(n) < 0$ for the CFW medium for $\lambda_0 \in [445, 535]$ nm [6, 7]. CFW disputed this alternative view [8, 9].

In order to resolve the issue, two studies were undertaken. First, following a procedure adopted by Wang and Lakhtakia [11], we performed a time–domain calculation that did not explicitly invoke the frequency–domain concept of refractive index. We used a finite–difference algorithm to solve the time–domain Maxwell equations for a pulsed plane wave reflected, at normal incidence, from a half–space filled with the CFW medium. Then we transformed the time–domain electric field of the reflected pulse to the frequency domain and computed the reflectance as a function of λ_0. Second, in the frequency domain, we considered a Gaussian beam propagating through a slab of the CFW medium at an oblique angle. The reflection and transmission coefficients were computed — without utilizing the refractive index — by solving the reflection–transmission problem as a boundary–value problem, and the deflection of the transmitted beam with respect to the incident beam was determined.

2 Time–domain analysis

Let us begin with the time–domain study. Suppose the CFW medium occupies the half–space $z > z_L$, ($z_L > 0$), and possesses the time–domain relative permittivity

$$\epsilon(t) = \delta(t) + \sum_{\ell=1}^{2} \alpha_\ell \omega_\ell \exp(-\beta_\ell \omega_\ell t) \sin(\omega_\ell t) \mathcal{U}(t), \tag{2}$$

where $\delta(t)$ is the Dirac delta function, $\mathcal{U}(t)$ is the unit step function; note that

$$\tilde{\epsilon}(\omega) = \int_{-\infty}^{\infty} \epsilon(t) \exp(i\omega t)\, dt. \tag{3}$$

The other half–space $z < z_L$ is vacuous.

A pulsed plane wave propagating in the $+z$ direction is introduced at $z = 0$, so that for $t > 0$

$$\mathbf{E}(z=0,t) = \hat{\mathbf{x}} \left(\frac{\eta_0 U_t}{\tau_0 \sqrt{\pi}}\right)^{\frac{1}{2}} \exp\left[-\left(\frac{t-t_d}{\sqrt{2}\tau_0}\right)^2\right] \cos(\omega_c t). \tag{4}$$

The electric field $\mathbf{E}(z,t) = \hat{\mathbf{x}}\, E(z,t)$ is polarized along the x axis, the magnetic field $\mathbf{H}(z,t) = \hat{\mathbf{y}}\, H(z,t)$ is polarized along the y axis, $\eta_0 = \sqrt{\mu_0/\epsilon_0}$ is the intrinsic impedance of free space (permittivity ϵ_0 and permeability μ_0), $c_0 = 1/\sqrt{\epsilon_0 \mu_0}$ is the speed of light in free space, U_t sets the energy density of the pulse, τ_0 is the time constant, t_d the time delay, and ω_c the carrier frequency.

Upon writing the components of the electromagnetic field in a column 2–vector as $[\underline{F}(z,t)] = [E(z,t), H(z,t)]^T$, where the superscript ^{T} indicates the transpose, and substituting the foregoing expressions for $\epsilon(t)$ into the Maxwell curl postulates, we found the matrix partial differential equation

$$\partial_t [\underline{F}(z,t)] = c_0 \left[\underline{\underline{V}}\right] \partial_z [\underline{F}(z,t)] - \epsilon_0^{-1} \partial_t \left[\underline{Q}(z,t)\right] \tag{5}$$

for $z, t > 0$. In this equation,

$$\left[\underline{\underline{V}}\right] = \begin{bmatrix} 0 & -\eta_0 \\ -1/\eta_0 & 0 \end{bmatrix} \tag{6}$$

is the vacuum propagation matrix, the column vector

$$\left[\underline{Q}(z,t)\right] = \epsilon_0 \int_0^t \left[\underline{\underline{W}}(z,t')\right] \left[\underline{F}(z,t-t')\right] dt', \tag{7}$$

and the matrix $\left[\underline{\underline{W}}(z,t)\right]$ is null–valued for $z < z_L$, but

$$\left[\underline{\underline{W}}(z,t)\right] = \begin{bmatrix} \epsilon(t) - \delta(t) & 0 \\ 0 & 0 \end{bmatrix}. \tag{8}$$

for $z > z_L$. The upper limit on the right side of eqn. (7) accounts for $[\underline{F}(z,t)]$ being null–valued for $t \leq 0$.

We computed the spatiotemporal evolution of the pulsed plane wave over the domain $\{(z,t) | z \in [0, z_R], z_R > z_L, t > 0\}$, which was discretized into space steps of length Δz and time steps of duration $\Delta t = \beta \Delta z / c_0$, where $\beta < 1$ is a stability parameter. We discretized eqn. (5) and solved

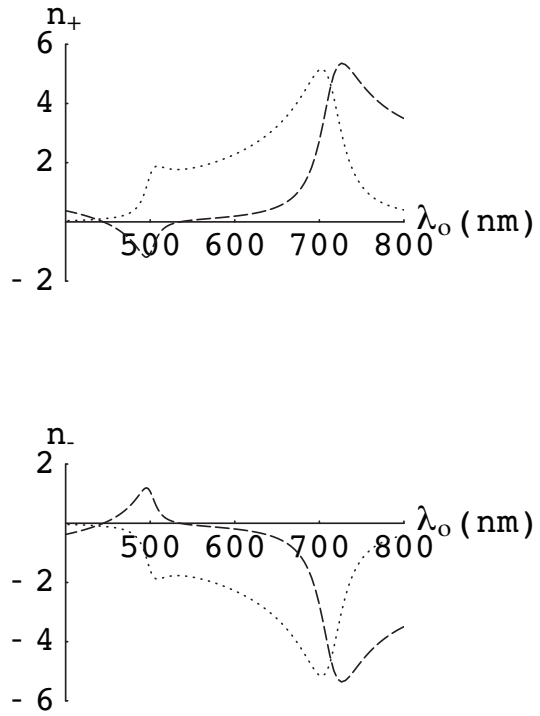

Figure 2: Real (dashed) and imaginary (dotted) parts of the indexes of refraction, as defined in the frequency domain.

it using over the chosen domain using a leapfrog finite–difference algorithm. Further details of our solution procedure are reported elsewhere [10].

We chose $z_0 = 0$ μm, $z_L = 20$ μm, and $z_R = 40$ μm. The electric field of the incident pulse $E_i(t)$ was recorded at $z = 0$ μm, and that of the reflected pulse $E_r(t)$ at $z = 18$ μm. The incident pulse had the parameters $U_t = 1$ J m^{-1}, $\tau_0 = 1$ fs, $t_d = 5$ fs, and $\omega_c = 3.8838 \times 10^{15}$ rad s^{-1}, so that its bandwidth was centered at the free–space wavelength $\lambda_0 = 485$ nm with a full–width half–maximum of about 220 nm. Then, we used the fast Fourier transform (FFT) to approximate the corresponding phasors $\tilde{E}_i(\lambda_0)$ and $\tilde{E}_r(\lambda_0)$ and found the reflectance from the time–domain calculations as

$$R_t(\lambda_0) = \left| \tilde{E}_r(\lambda_0) \left[\tilde{E}_i(\lambda_0) \right]^{-1} \right|^2 . \tag{9}$$

There are two possibilities for the refractive index n, *viz.*, $n_\pm$ such that $n_- = -n_+$ and $\mathrm{Im}(n_+) > 0$. Plots of $\mathrm{Re}(n_\pm)$ and $\mathrm{Im}(n_\pm)$ as functions of λ_0 are shown in Fig. 2. From these two possibilities, we found the frequency–domain reflectances

$$R_\pm(\lambda_0) = \left| [n_\pm(\lambda_0) - 1] [n_\pm(\lambda_0) + 1]^{-1} \right|^2 \tag{10}$$

for plane waves normally incident on a half–space. As $R_+ R_- = 1$, R_t can be used to distinguish between them if $R_\pm \neq 1$ [11].

Plots of R_t, R_+, and R_- vs. λ_0 are shown in Fig. 3 over the bandwidth covered by the incident pulse. As $|R_t| > 1$ over at least part of that bandwidth, the CFW medium is active over that

part of that bandwidth. However, we found that neither the pulse reflected from nor the pulse refracted into the medium grew unboundedly. Furthermore, as the reflectance R_t obtained from the time–domain calculations closely matches R_+, the refractive index with positive imaginary part (i.e., n_+) is the correct one.

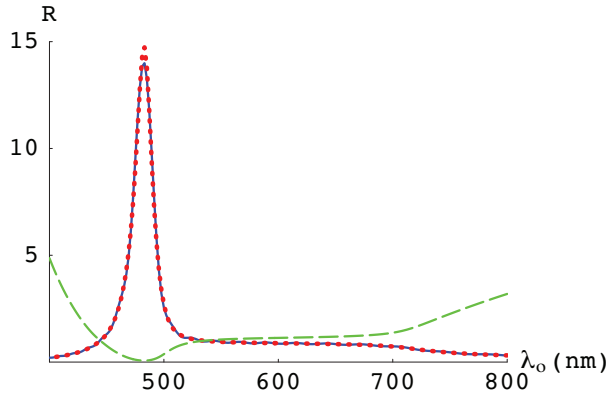

Figure 3: Reflectances R_t (blue solid), R_+ (red dotted), and R_- (green dashed).

3 Frequency–domain analysis

Next we turn to the frequency–domain study which does not require the specification of n as either n_- or n_+. Suppose that the half–space is now replaced by a slab of thickness L, as schematically illustrated in Fig. 4. The slab — which consists of dielectric material with relative permittivity defined in eqn. (1) — is sandwiched by two vacuous half–spaces.

A 2D beam with electric field phasor [12]

$$\tilde{\mathbf{E}}_i(x,z,\lambda_0) = \int_{-\infty}^{\infty} \mathbf{e}_i(\vartheta)\,\Psi(\vartheta)\,e^{i\mathbf{k}_+(\vartheta)\cdot\mathbf{r}}\,d\vartheta, \tag{11}$$

for $z \leq 0$, is incident upon the slab at a mean angle θ_i relative to the slab normal direction $\hat{\boldsymbol{z}}$. The beam is represented as an angular spectrum of plane waves, with

$$\begin{aligned}\mathbf{k}_\pm(\vartheta) &= k_0\Big[\left(\vartheta\,\cos\theta_i + \sqrt{1-\vartheta^2}\,\sin\theta_i\right)\hat{\mathbf{x}} \\ &\quad \mp \left(\vartheta\,\sin\theta_i - \sqrt{1-\vartheta^2}\,\cos\theta_i\right)\hat{\mathbf{z}}\Big],\end{aligned} \tag{12}$$

where $k_0 = 2\pi/\lambda_0$. The angular–spectral function $\Psi(\vartheta)$ is taken to have the Gaussian form [12]

$$\Psi(\vartheta) = \frac{k_0\,w_0}{\sqrt{2\pi}}\,\exp\left[-\frac{1}{2}\,(k_0\,w_0\,\vartheta)^2\right], \tag{13}$$

with w_0 being the width of the beam waist. Two polarization states are considered: parallel to the plane of incidence, i.e.,

$$\begin{aligned}\mathbf{e}_i(\vartheta) \equiv \mathbf{e}_\parallel &= \left(\vartheta\,\sin\theta_i - \sqrt{1-\vartheta^2}\,\cos\theta_i\right)\hat{\mathbf{x}} \\ &\quad + \left(\vartheta\,\cos\theta_i + \sqrt{1-\vartheta^2}\,\sin\theta_i\right)\hat{\mathbf{z}}\end{aligned} \tag{14}$$

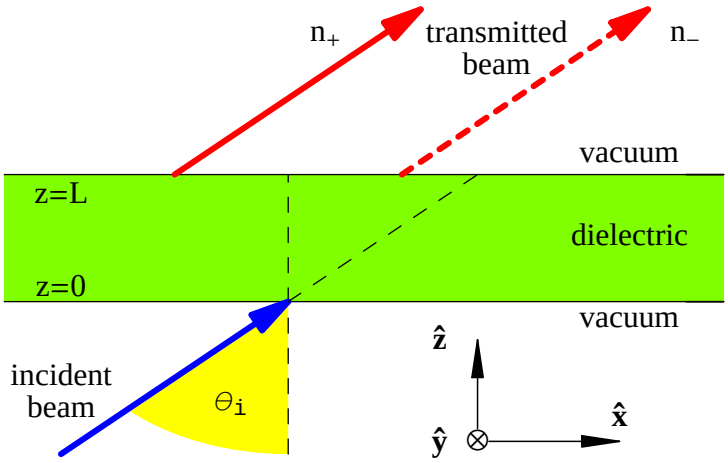

Figure 4: A beam is incident onto a slab at a mean angle θ_i with respect to the unit vector $\hat{\mathbf{z}}$ normal to the planar interface. The incident beam strikes the slab at the coordinate origin (i.e., $x = 0, y = 0$ and $z = 0$). The transmitted beam emerges from the slab at $z = L$ at a point with (a) $x > 0$ if the refractive index of the slab is positive (dashed red arrow); or (b) $x < 0$ if the refractive index of the slab is negative (solid red arrow).

and perpendicular to the plane of incidence, i.e.,

$$\mathbf{e}_i(\vartheta) \equiv \mathbf{e}_\perp = \hat{\mathbf{y}}. \tag{15}$$

As the incident beam has the spatial Fourier representation (11), the reflected and the transmitted beams must also have similar representations. The electric field phasor of the reflected beam is given as

$$\tilde{\mathbf{E}}_r\,(x, z, \lambda_0) = \int_{-\infty}^{\infty} \mathbf{e}_r(\vartheta)\,\Psi(\vartheta)\,e^{i\mathbf{k}_-(\vartheta)\cdot\mathbf{r}}\,d\vartheta, \tag{16}$$

for $z \leq 0$, with

$$\mathbf{e}_r(\vartheta) = \begin{cases} r_\parallel\Big[-\Big(\vartheta\,\sin\theta_i - \sqrt{1-\vartheta^2}\,\cos\theta_i\Big)\,\hat{\mathbf{x}} \\ \quad + \Big(\vartheta\,\cos\theta_i + \sqrt{1-\vartheta^2}\,\sin\theta_i\Big)\,\hat{\mathbf{z}}\Big] \\ \qquad \text{for} \quad \mathbf{e}_i(\vartheta) = \mathbf{e}_\parallel \\ r_\perp\,\mathbf{e}_\perp \quad \text{for} \quad \mathbf{e}_i(\vartheta) = \mathbf{e}_\perp \end{cases}. \tag{17}$$

The electric field phasor of the transmitted beam is given as

$$\tilde{\mathbf{E}}_t\,(x, z, \lambda_0) = \int_{-\infty}^{\infty} \mathbf{e}_t(\vartheta)\,\Psi(\vartheta)\,e^{i\mathbf{k}_+(\vartheta)\cdot(\mathbf{r}-L\hat{\mathbf{z}})}\,d\vartheta, \tag{18}$$

for $z \geq L$, with

$$\mathbf{e}_t(\vartheta) = \begin{cases} t_\parallel\,\mathbf{e}_i(\vartheta) & \text{for} \quad \mathbf{e}_i(\vartheta) = \mathbf{e}_\parallel \\ t_\perp\,\mathbf{e}_\perp & \text{for} \quad \mathbf{e}_i(\vartheta) = \mathbf{e}_\perp \end{cases}. \tag{19}$$

The reflection coefficients $r_{\parallel,\perp}$ and transmission coefficients $t_{\parallel,\perp}$ were calculated as functions of ϑ by solving a boundary–value problem [13], as described in the Appendix.

We fixed the mean angle of incidence $\theta_i = 60^\circ$, the free–space wavelength $\lambda_0 = 485$ nm, the beam waist $w_0 = 1.75\lambda_0$, and the slab thickness $L = 4\lambda_0$. The restriction $\vartheta \in [-1, 1]$ was imposed to exclude evanescence. The numerical values for the beam waist and slab thickness were chosen in order to accentuate the clarity of Fig. 5, which shows the energy density in both half–spaces, as defined by

$$|\tilde{\mathbf{E}}|^2 = \begin{cases} |\tilde{\mathbf{E}}_i + \tilde{\mathbf{E}}_r|^2 & \text{for} \quad z \leq 0 \\ |\tilde{\mathbf{E}}_t|^2 & \text{for} \quad z \geq L \end{cases} , \tag{20}$$

for $z/\lambda_0 \in (-8, 12)$ and $x/\lambda_0 \in (-25, 25)$.

As illustrated in Fig. 1, at $\lambda_0 = 485$ nm the relative permittivity of the CFW material is $\tilde{\epsilon} = 0.51 - 0.87i$. The corresponding reflection and transmission coefficients were numerically determined at $\vartheta = 0$ as $r_\parallel = -3.16 + 0.58i$, $r_\perp = -1.14 - 1.31i$, $t_\parallel = (3.69 + 3.66i) \times 10^{-8}$ and $t_\perp = (-1.82 - 0.10) \times 10^{-8}$. In order to make visible the tiny fraction of the beam that is transmitted, the values of $|\tilde{\mathbf{E}}_t|^2$ in Fig. 5 have been amplified by a factor of 5×10^{14} for $\mathbf{e}_i = \mathbf{e}_\parallel$, and by a factor of 3×10^{15} for $\mathbf{e}_i = \mathbf{e}_\perp$. The fact that the CFW medium is active at $\lambda_0 = 485$ nm is clear from $|r_\parallel|^2 > 1$ and $|r_\perp|^2 > 1$ (in fact, $|r_\parallel|^2 = 10.32$ and $|r_\perp|^2 = 3.00$).

From Fig. 5 we conclude that the beam undergoes negative refraction at the two interfaces between the CFW slab and free space. While this occurs for both polarization states, it is more noticeable for the parallel polarization state.

4 Concluding remarks

In conclusion, there is an ambiguity inherent in the frequency–domain concept of refractive index, concerning the choice of square root. This pertains to both the bending of light at planar interfaces and the determination of whether the medium under consideration is active or passive. Using (i) a time–domain method and (ii) a frequency–domain method, neither of which explicitly invokes the refractive index, we resolved these issues for the two–component CFW medium characterized by the relative permittivity given in eqn. (1). The CFW medium was found to be (a) an active medium — contrary to the claims of CFW [1]; and (b) negatively refracting — contrary to other recent claims [6, 7].

Acknowledgements: We thank S. A. Ramakrishna for helpful discussions. JBG is supported by a *Beckman Postdoctoral Fellowship*. TGM is supported by a *Royal Society of Edinburgh/Scottish Executive Support Research Fellowship*.

Appendix

The reflection coefficients $r_{\parallel,\perp}$ and transmission coefficients $t_{\parallel,\perp}$ are straightforwardly calculated by solving a boundary–value problem as follows [13].

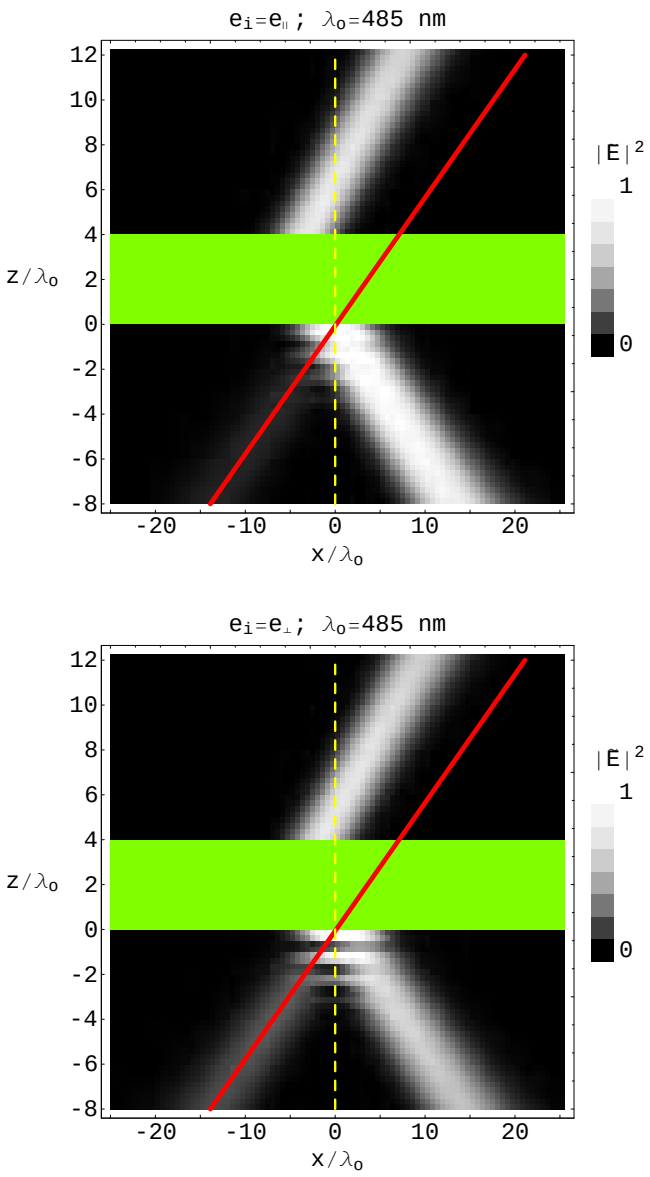

Figure 5: Normalized $|\tilde{\mathbf{E}}|^2$ is mapped in the xz plane for a 2D Gaussian beam incident onto a CFW dielectric slab at a mean angle $\theta_i = 60°$. $\tilde{\mathbf{E}}_i$ is polarized parallel (top) and perpendicular (bottom) to the plane of incidence. The red line indicates the mean beam position in the absence of the dielectric slab.

Consider the plane wave with electric and magnetic field phasors

$$\left.\begin{aligned} \tilde{\mathbf{E}}(x,z) &= \tilde{\mathbf{e}}(z,\theta)\, \exp\left(ik_0 x \sin\theta\right) \\ \tilde{\mathbf{H}}(x,z) &= \tilde{\mathbf{h}}(z,\theta)\, \exp\left(ik_0 x \sin\theta\right) \end{aligned}\right\} \tag{21}$$

propagating in the xz plane and incident on a dielectric slab with relative permittivity $\tilde{\epsilon}$ occupying

the region between $z = 0$ and $z = L$. The angle θ is related to the mean angle θ_i of a Gaussian beam and the parameter ϑ by the twin relations

$$\left.\begin{aligned} \sin\theta &= \vartheta\,\cos\theta_i + \sqrt{1-\vartheta^2}\,\sin\theta_i \\ \cos\theta &= -\vartheta\,\sin\theta_i + \sqrt{1-\vartheta^2}\,\cos\theta_i \end{aligned}\right\}. \tag{22}$$

Substitution of eqn. (21) into the source–free Maxwell curl postulates $\nabla\times\tilde{\mathbf{E}}(x,z) - i\omega\mu_0\tilde{\mathbf{H}}(x,z) = \mathbf{0}$ and $\nabla\times\tilde{\mathbf{H}}(x,z) + i\omega\epsilon_0\tilde{\epsilon}\tilde{\mathbf{E}}(x,z) = \mathbf{0}$ delivers four differential equations and two algebraic equations. The latter two equations are easily solved for $\tilde{e}_z$ and $\tilde{h}_z$. Thereby, the four differential equations may be expressed in matrix form as

$$\frac{\partial}{\partial z}\left[\,\underline{\tilde{f}}(z,\theta)\right] = ik_0\left[\,\underline{\underline{\tilde{P}}}(\theta)\right]\left[\,\underline{\tilde{f}}(z,\theta)\right], \tag{23}$$

where

$$\left[\,\underline{\tilde{f}}(z,\theta)\right] = \left[\,\tilde{e}_x(z,\theta),\,\tilde{e}_y(z,\theta),\,\tilde{h}_x(z,\theta),\,\tilde{h}_y(z,\theta)\right]^T \tag{24}$$

is a column vector and

$$\left[\,\underline{\underline{\tilde{P}}}(\theta)\right] = \begin{bmatrix} 0 & 0 & 0 & \eta_0\rho \\ 0 & 0 & -\eta_0 & 0 \\ 0 & -\tilde{\epsilon}\rho/\eta_0 & 0 & 0 \\ \tilde{\epsilon}/\eta_0 & 0 & 0 & 0 \end{bmatrix} \tag{25}$$

is a 4×4 matrix with

$$\rho = 1 - \frac{\sin^2\theta}{\tilde{\epsilon}}. \tag{26}$$

The solution to eqn. (23) is conveniently expressed as

$$\left[\,\underline{\tilde{f}}(L,\theta)\right] = \left[\,\underline{\underline{\tilde{M}}}(L,\theta)\right]\left[\,\underline{\tilde{f}}(0,\theta)\right], \tag{27}$$

in terms of the transfer matrix [13]

$$\left[\,\underline{\underline{\tilde{M}}}(L,\theta)\right] = \sum_{\ell=0}^{\infty}\frac{1}{\ell!}\left\{ik_0\left[\,\underline{\underline{\tilde{P}}}(\theta)\right]\,L\right\}^{\ell}. \tag{28}$$

Since the evaluation of $\left[\,\underline{\underline{\tilde{M}}}(L,\theta)\right]$ as a power series does not invoke the refractive index, ambiguities associated with the determining the correct square root of $\tilde{\epsilon}$ are avoided.

Now we turn to the incident, reflected and transmitted plane waves. Let the incident plane wave be represented in terms of linear polarization components as

$$\left.\begin{aligned} \tilde{\mathbf{e}}_i(z,\theta) &= \left[a_\perp\,\hat{\mathbf{y}} + a_\parallel\,(\sin\theta\,\hat{\mathbf{z}} - \cos\theta\,\hat{\mathbf{x}})\right] \\ &\qquad\times\exp\left(ik_0 z\cos\theta\right) \\ \tilde{\mathbf{h}}_i(z,\theta) &= \left[a_\perp\,(\sin\theta\,\hat{\mathbf{z}} - \cos\theta\,\hat{\mathbf{x}}) - a_\parallel\,\hat{\mathbf{y}}\,\right] \\ &\qquad\times\eta_0^{-1}\,\exp\left(ik_0 z\cos\theta\right) \end{aligned}\right\}, z \le 0. \tag{29}$$

The corresponding reflected and transmitted plane waves are given as

$$\left.\begin{aligned} \tilde{\mathbf{e}}_r(z,\theta) &= \left[a_\perp r_\perp\,\hat{\mathbf{y}} + a_\parallel r_\parallel\,(\cos\theta\,\hat{\mathbf{x}} + \sin\theta\,\hat{\mathbf{z}})\right] \\ &\qquad\times\exp\left(-ik_0 z\cos\theta\right) \\ \tilde{\mathbf{h}}_r(z,\theta) &= \left[a_\perp r_\perp\,(\cos\theta\,\hat{\mathbf{x}} + \sin\theta\,\hat{\mathbf{z}}) - a_\parallel r_\parallel\,\hat{\mathbf{y}}\,\right] \\ &\qquad\times\eta_0^{-1}\,\exp\left(-ik_0 z\cos\theta\right) \end{aligned}\right\}, z \le 0 \tag{30}$$

and

$$\left.\begin{array}{rl} \tilde{\mathbf{e}}_t(z,\theta) = & \left[a_\perp t_\perp \,\hat{\mathbf{y}} + a_\parallel t_\parallel \,(\sin\theta\,\hat{\mathbf{z}} - \cos\theta\,\hat{\mathbf{x}})\right] \\ & \times \exp\left[ik_0(z-L)\cos\theta\right] \\ \tilde{\mathbf{h}}_t(z,\theta) = & \left[a_\perp t_\perp \,(\sin\theta\,\hat{\mathbf{z}} - \cos\theta\,\hat{\mathbf{x}}) - a_\parallel t_\parallel \,\hat{\mathbf{y}}\,\right] \\ & \times \eta_0^{-1} \exp\left[ik_0(z-L)\cos\theta\right] \end{array}\right\}, z \geq L, \tag{31}$$

respectively. By application of the boundary conditions at $z = 0$ and $z = L$ to the solution (27), the reflection and transmission coefficients are found to be related by the matrix algebraic equation

$$\left[\underline{\underline{K}}(\theta)\right]\left[t_\perp, t_\parallel, 0, 0\right]^T = \left[\underline{\underline{\tilde{M}}}(L,\theta)\right]\left[\underline{\underline{K}}(\theta)\right]\left[1, 1, r_\perp, r_\parallel\right]^T, \tag{32}$$

wherein

$$\left[\underline{\underline{K}}(\theta)\right] = \left[\begin{array}{cccc} 0 & -\cos\theta & 0 & \cos\theta \\ 1 & 0 & 1 & 0 \\ -\eta_0^{-1}\cos\theta & 0 & \eta_0^{-1}\cos\theta & 0 \\ 0 & -\eta_0^{-1} & 0 & -\eta_0^{-1} \end{array}\right]. \tag{33}$$

Thus, the reflection and transmission coefficients emerge as components of the 4×4 matrix

$$\left[\underline{\underline{\tilde{S}}}\right] = \left[\underline{\underline{K}}(\theta)\right]^{-1}\left[\underline{\underline{\tilde{M}}}(L,\theta)\right]\left[\underline{\underline{K}}(\theta)\right], \tag{34}$$

as per

$$r_\perp = -\left[\underline{\underline{\tilde{S}}}\right]_{31}\left(\left[\underline{\underline{\tilde{S}}}\right]_{33}\right)^{-1}, \tag{35}$$

$$r_\parallel = -\left[\underline{\underline{\tilde{S}}}\right]_{42}\left(\left[\underline{\underline{\tilde{S}}}\right]_{44}\right)^{-1}, \tag{36}$$

$$t_\perp = \left[\underline{\underline{\tilde{S}}}\right]_{11} - \left[\underline{\underline{\tilde{S}}}\right]_{13}\left[\underline{\underline{\tilde{S}}}\right]_{31}\left(\left[\underline{\underline{\tilde{S}}}\right]_{33}\right)^{-1}, \tag{37}$$

$$t_\parallel = \left[\underline{\underline{\tilde{S}}}\right]_{22} - \left[\underline{\underline{\tilde{S}}}\right]_{24}\left[\underline{\underline{\tilde{S}}}\right]_{42}\left(\left[\underline{\underline{\tilde{S}}}\right]_{44}\right)^{-1}. \tag{38}$$

References

[1] Y–F. Chen, P. Fischer, F.W. Wise, Phys. Rev. Lett. 95 (2005) 067402.

[2] J. Skaar, Phys. Rev. E 73 (2006) 026605.

[3] J. Skaar, Opt. Lett. 31 (2006) 3372.

[4] S.A. Ramakrishna, O.J. Martin, Opt. Lett. 30 (2005), 2626.

[5] J. Wei, M. Xiao, Opt. Commun. 270 (2007) 455.

[6] T.G. Mackay, A. Lakhtakia, Phys. Rev. Lett. 96 (2006) 159701.

[7] S.A. Ramakrishna, Phys. Rev. Lett. 98 (2007) 059701.

[8] Y–F. Chen, P. Fischer, F.W. Wise, Phys. Rev. Lett. 96 (2006) 159702.

[9] Y–F. Chen, P. Fischer, F.W. Wise, Phys. Rev. Lett. 98 (2007) 059702.

[10] J.B. Geddes III, A. Lakhtakia, J. Mod. Opt. 53 (2006) 2763.

[11] J. Wang, A. Lakhtakia, Microwave Opt. Technol. Lett. 33 (2002) 465.

[12] H.A. Haus, Waves and fields in optoelectronics, Prentice–Hall, Englewood Cliffs, NJ, USA, 1984.

[13] A. Lakhtakia, R. Messier, Sculptured thin films: Nanoengineered optics and morphology, SPIE Press, Bellingham, WA, USA, 2005.